

Organic Anions. Part 12.¹ Hard Sphere Electrostatic Calculations on Group 1 Organometallic Compounds: Ion Pairs of Dianions and Radical Anions

Richard J. Bushby* and Helen L. Steel
School of Chemistry, The University, Leeds, LS2 9JT

Hard Sphere Electrostatic (HSE) calculations on the structure of the dilithium salts of the dianions of benzene, naphthalene, anthracene, phenanthrene, acenaphthalene, stilbene, and hexatriene ($R^{2-}, 2Li^+$) are compared with known crystal structures and the results of MO calculations. The HSE method is then used to predict the structures of other species for which no structural data are available, *i.e.* R^{2-}, Li^+ ; R^{2-}, Cs^+ ; R^{2-}, SS^+ ; $R^{2-}, 2Cs^+$; $R^{2-}, 2SS^+$; R^{2-}, Li^+, Cs^+ ; and R^{2-}, Li^+, SS^+ where R^{2-} represents the same series of dianions and SS^+ is the abbreviation used for the counterion in a solvent-separated ion pair. Whereas the sites adopted by the lithium cations in $R^{2-}, 2Li^+$ rarely correspond to those found in R^-, Li^+ the main minima for $R^{2-}, 2Li^+$ are mostly combinations of those found in the single counterion case R^{2-}, Li^+ . This is a reflection of the greater importance of anion/cation attraction and lesser importance of cation/cation repulsion in these dianions. Calculations are also reported for the structures of ion pairs ($M^+ = Li^+, Cs^+, SS^+$) of the radical anions of benzene, naphthalene, anthracene, phenanthrene, stilbene, and hexatriene, and for some ion pairs of dications R^{2+}, X^- ; $R^{2+}, 2X^-$ and radical cations R^+, X^- .

In previous papers in this series^{1,2} a simple (HSE) method was developed with the aim of predicting the structures of organic ion pairs. The method was used to predict the structures of 1:1 ion pairs, R^-, M^+ (where R^- represents a delocalised organic anion and M^+ is a group 1 cation) and 1:2 triple ions, $R^-, 2M^+$. Although the data for 1:1 ion pairs could be compared with known crystal structures and with the results of MO calculations, no such comparison was possible for the triple ions. The required data on triple ions do, however, exist for organic dianions, $R^{2-}, 2M^+$. The existence of such dianions is remarkable. When it is considered that most organic monoanions are unstable towards electron loss ($R^- \longrightarrow R^+ +$

e^-)³ the same must certainly be true of dianions and yet they are common organic intermediates.^{4,5} Their existence in solution bears witness to the remarkable stabilising power of ionic interactions^{4,6} and in this paper it is shown that it is these same interactions that dominate their structural chemistry.

The Benzene Dianion.—Although dianion intermediates are sometimes written for the reduction of benzene derivatives the dianion of benzene itself is unknown. It would be an eight-electron 'antiaromatic' system and might well have a triplet ground state. For the HSE calculations a symmetrical planar benzene ring was used with a charge of $-\frac{1}{2}$ on each carbon. The

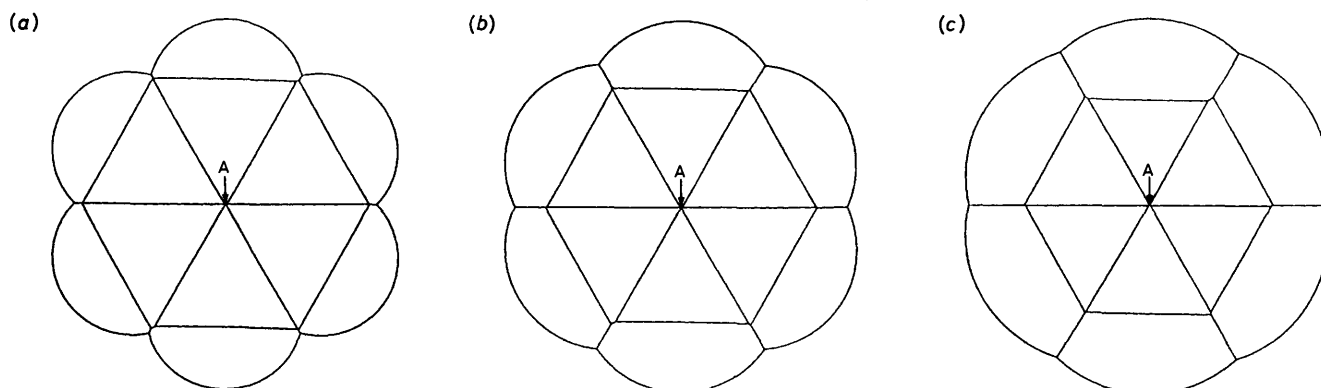


Figure 1. Ion-pair surfaces and associated HSE minima for the Li^+ , Cs^+ , and SS^+ ion pairs of $benzene^{2-}$. (SS^+ is the abbreviation used for the counter-ion in a solvent-separated ion pair and was modelled on $Li^+, 4THF$.) The ion-pair surface is that defined by the nucleus of the cation as it rolls over the surface of the anion. Drawn to scale the SS^+ ion-pair surface would be much larger than that for the Li^+ ion pair but for ease of display and comparison the surfaces have been scaled. All surfaces were searched by the automated x/y -plane search procedure and minima checked by inspection of suitably magnified contour plots or pair of contour plots are described in ref. 1. Since this particular dianion geometry is planar \bar{A} lies directly below A (a bar is always used to indicate a point on the lower surface). Energies are expressed in the form $E-\epsilon$ in $kcal\ mol^{-1}$, *i.e.*, for media other than a vacuum the energies should be divided by the effective microscopic relative permittivity. HMO charge distributions have been used throughout.

$benzene^{2-}, Li^+$ [Figure 1(a)] a minimum at A, \bar{A} , 292.1 (*i.e.* for the monolithium salt there are two equal, degenerate minima with an energy of $-292.1\ kcal\ mol^{-1}$); no local minima. $benzene^{2-}, 2Li^+$ [Figure 1(a)] minimum at A, \bar{A} , 491.7 (*i.e.* for the dilithium salt the minimum has one lithium at A and the other at \bar{A}); no local minima. $benzene^{2-}, Cs^+$ [Figure 1(b)] minimum at A, \bar{A} , 195.7; no local minima. $benzene^{2-}, 2Cs^+$ [Figure 1(b)] minimum at A, \bar{A} , 337.8; no local minima. $benzene^{2-}, SS^+$ [Figure 1(c)] minimum at A, \bar{A} , 107.1; no local minima. $benzene^{2-}, 2SS^+$ [Figure 1(c)] minimum at A, \bar{A} , 186.7; no local minima. $benzene^{2-}, Li^+, Cs^+$ [Figures 1(a) and 1(b)] minimum at A [Figure 1(a)]– \bar{A} [Figure 1(b)], $\bar{A}-A$, 419.9 (*i.e.* two degenerate minima in the first the lithium is at point A on surface 1(a) and the caesium at point \bar{A} on surface 1(b). The two surfaces should be considered as co-centred); no local minima. $benzene^{2-}, Li^+, SS^+$ [Figures 1(a) and 1(c)] minimum at A [Figure 1(a)]– \bar{A} [Figure 1(c)], $\bar{A}-A$, 356.8; no local minima.

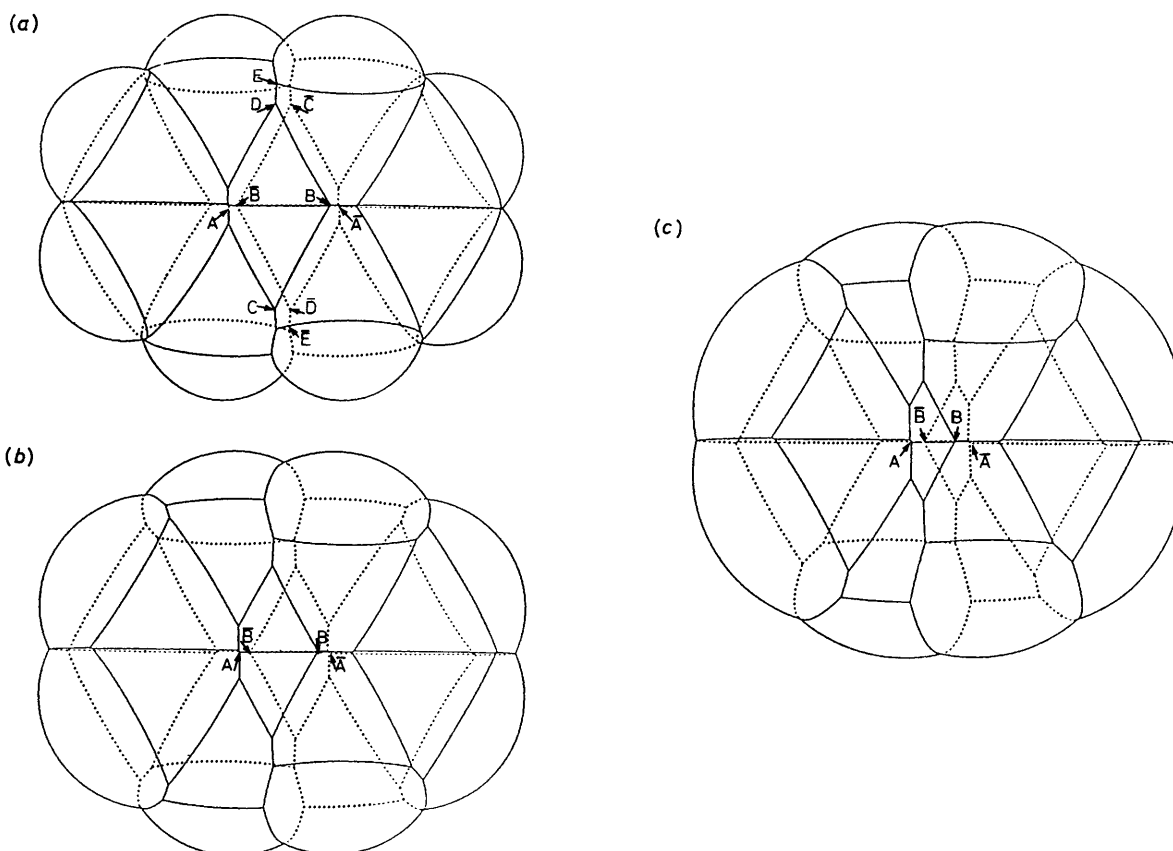


Figure 2. Ion-pair surfaces and associated HSE minima for the Li^+ , Cs^+ , and SS^+ ion pairs of naphthalene $^{2-}$. The anion is non-planar. Discontinuities on the lower surface are shown by the dashed lines and as usual points on the lower surface are distinguished by a bar. X is related to \bar{X} by an inversion centre. The other terms used are explained in the heading to Figure 1. HMO charge distributions were used in each case.

Naphthalene $^{2-}$, Li^+ [Figure 2(a)] minimum at A, \bar{A} , 237.1; local minima at B, \bar{B} , 236.9; C, \bar{C} , 212.4; D, \bar{D} , 212.2; no further local minima. *Naphthalene* $^{2-}$, 2Li^+ [Figure 2(a)] minimum at A- \bar{A} , 397.0; local minima at B- \bar{B} , 396.7; A- \bar{B} , B- \bar{A} , 384.6; C- \bar{C} , 365.6; D- \bar{D} , 365.3; no further minima with cations on opposite faces; the best minimum with both cations on the same face is C-E, \bar{C} - \bar{E} , 352.0; further local minima of this type were not checked (*i.e.* they were found by the automated search but not checked by inspection of energy contour diagrams). *Naphthalene* $^{2-}$, Cs^+ [Figure 2(b)] minimum at A, \bar{A} , 173.2; local minima at B, \bar{B} , 173.0; no further local minima. *Naphthalene* $^{2-}$, 2Cs^+ [Figure 2(b)] minimum at A- \bar{A} , 296.2; local minima not checked. *Naphthalene* $^{2-}$, SS^+ [Figure 2(c)] minimum at A, \bar{A} , 102.4; local minima at B, \bar{B} , 102.3; no further local minima. *Naphthalene* $^{2-}$, 2SS^+ [Figure 2(c)], minimum at A- \bar{A} , 177.8; local minima not checked. *Naphthalene* $^{2-}$, Li^+ , Cs^+ [Figures 2(a) and (b)], minimum at A [Figure 2(a)]- \bar{A} [Figure 2(b)], \bar{A} -A, 349.1; local minima not checked. *Naphthalene* $^{2-}$, Li^+ , SS^+ [Figures 2(a) and (c)], minimum at A [Figure 2(a)]- \bar{A} [Figure 2(c)], \bar{A} -A, 298.9; local minima not checked.

results obtained (Figure 1) are very straightforward and mirror those for the cyclopentadienyl anion.¹ In all cases the minimum-energy structures have the cations in central (η^6) sites.

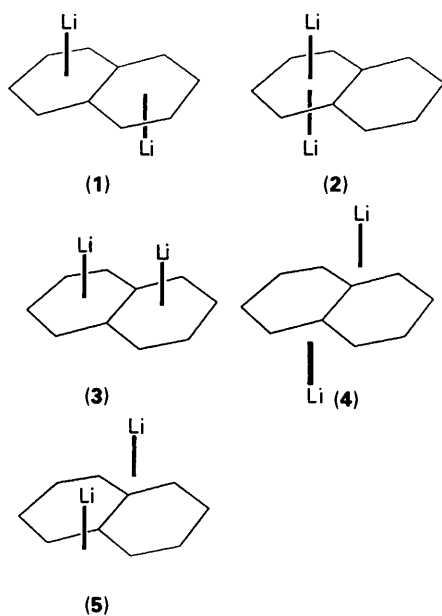
The Naphthalene Dianion.—Although from some standpoints the dianion of naphthalene can also be regarded as ‘antiaromatic’ it is well known. The dilithium salt can be isolated as its tetramethylethylene diamine complex⁷ and its X-ray crystal structure has been determined by Stucky and co-workers. In this structure, one lithium is above one ring and the other below the other ring [as in formula (1), corresponding to positions B and \bar{B} in Figure 2(a)]. This and the other two obvious bis- η^6 structures (2) and (3) were considered by Sygula *et al.* as start points for their MNDO-MO calculations.⁸ They ranked these in order of stability (1) > (2) > (3). They claim that electrostatic methods (unspecified) predict a minimum with one lithium above and one below the 4a-8a bond whereas use of a ‘sparkle’ predicts a minimum with one above and one below atom 8a. These electrostatic minima predicted by Sygula are in disagreement with our HSE results. These agree, rather, with the crystal structure and they also serve to highlight further, unconsidered potential local energy minima.

For the HSE calculations Stucky’s geometry for the dianion⁷

was used together with an HMO charge distribution. For the 1:1 ion pairs naphthalene $^{2-}$, Li^+ , as well as the expected sites where the lithium is close to η^6 over the benzene rings, local minima were found in which the lithium η^3 bridges the *peri* positions [sites C, \bar{C} , D, \bar{D} in Figure 2(a)]. In retrospect these η^3 sites might have been expected since they represent the alternative way in which the cation can bridge the most highly charged centres in the dianion (the α -carbons). The minima found in the HSE calculation on the dilithium salt, naphthalene $^{2-}$, 2Li^+ , correspond to various ways of combining these η^6 and η^3 sites as shown in formulae (1)–(5). The ‘rank order’ of stabilities (1) > (2) > (4) > (3) agrees, in broad terms, with the results of Stucky and co-workers⁷ and the MO calculations of Sygula *et al.*⁸ [except that these authors do not seem to have considered structures analogous to formulae (4) and (5)].

The Anthracene Dianion.—The X-ray crystal structures of [anthracene $^{2-}$, 2Li^+ , $2\text{Me}_2\text{NCH}_2\text{CH}_2\text{NMe}_2$]⁹ and [anthracene $^{2-}$, Mg^{2+} , 3THF]^{10,*} are known and less direct evidence

* THF = tetrahydrofuran.

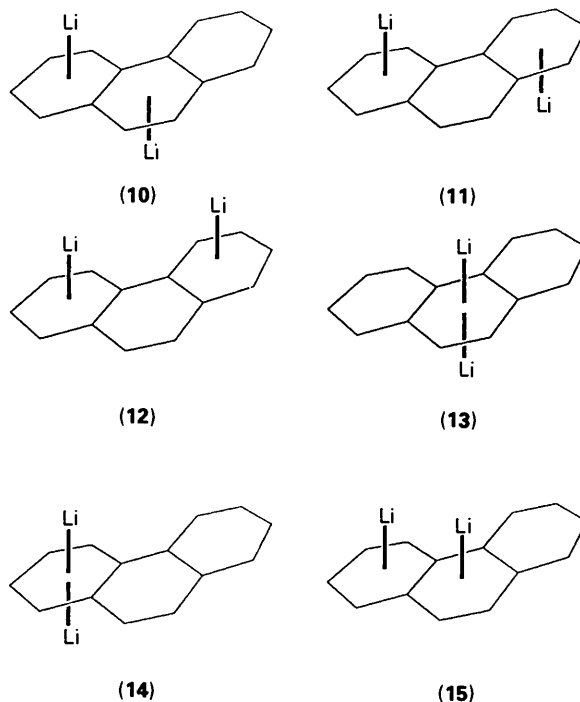
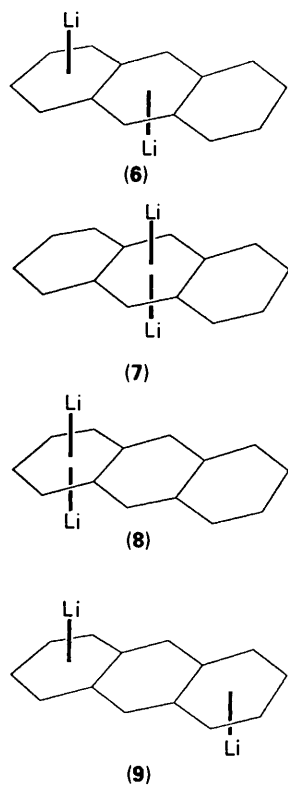


for the structure of the dilithium salt of anthracene dianion is provided by the MNDO-MO calculations of Sygula *et al.*⁸

For the HSE calculations the geometry chosen for the anion was that provided by Stucky's X-ray crystal structure⁹ and resultant ion-pair surfaces are shown in Figure 3. For the 1:1 lithium salt anthracene²⁻,Li⁺ calculations show minima with the cation above and below the six-membered rings. The best minimum, at position A [Figure 3(a)], corresponds to that found in the X-ray crystal structure of [anthracene²⁻,Mg²⁺,3THF].¹⁰ For the dilithium salt, anthracene²⁻,2Li⁺, the situation is more complex. If we assume that the lithiums are in η^6 sites and on opposite sides of the anion, four types of

structure are possible and these are shown in formula (6)–(9). As well as structures of these types, however, others are possible in which both of the lithiums are on the same side of the anion or where the lithiums adopt η^3 sites [analogous to those in formulae (4) and (5)]. This gives a very large number of potential structures. The X-ray crystal structure of [anthracene²⁻,2Li⁺,2Me₂NCH₂CH₂NMe₂]⁹ is analogous to that shown in formula (6). Sygula's MNDO calculations rank the four main structural types in order of stability (6) > (7) > (9) > (8). In the HSE calculations where the counterions are larger the results are unambiguous and give structures analogous to formula (7). For the dilithium salts, however, a large number of local minima are found which span a small energy range, and the ordering of these energy minima depends on the exact geometry and charge distribution chosen. For example, on picking out the structures analogous to those examined by Sygula *et al.*, the stability order is (7) > (6) > (9) > (8) if an HMO charge distribution is used, but is (9) > (6) > (7) > (8) if a CNDO-2 charge distribution is used. However, many 'structures' were found that were not considered in the MNDO study. The variability in ordering of local minima is something that is also found for the phenanthrene dianion dilithium salt and will be discussed at a later point, but it seems reasonable to conclude that when there are many such local minima spanning a small energy range neither MO nor HSE calculations can be relied on as a guide to the structure in solution.

The Phenanthrene Dianion.—Although the dianion of phenanthrene is a well known intermediate^{4,5} no X-ray crystal structure of any of its salts is available and the only guide as to where the counterions reside comes from the MNDO-MO calculations of Sygula *et al.*⁸ These workers only considered six possible structures for the dilithium salt, (10)–(15), which they ranked in stability order (10) > (11) > (12) > (13) > (14) > (15). They also report that use of a 'sparkle' in place of each lithium cation results in a structure equivalent to formula (13), with the charges on either side of the central ring. For the HSE calculations the geometry used was the near-planar geometry of



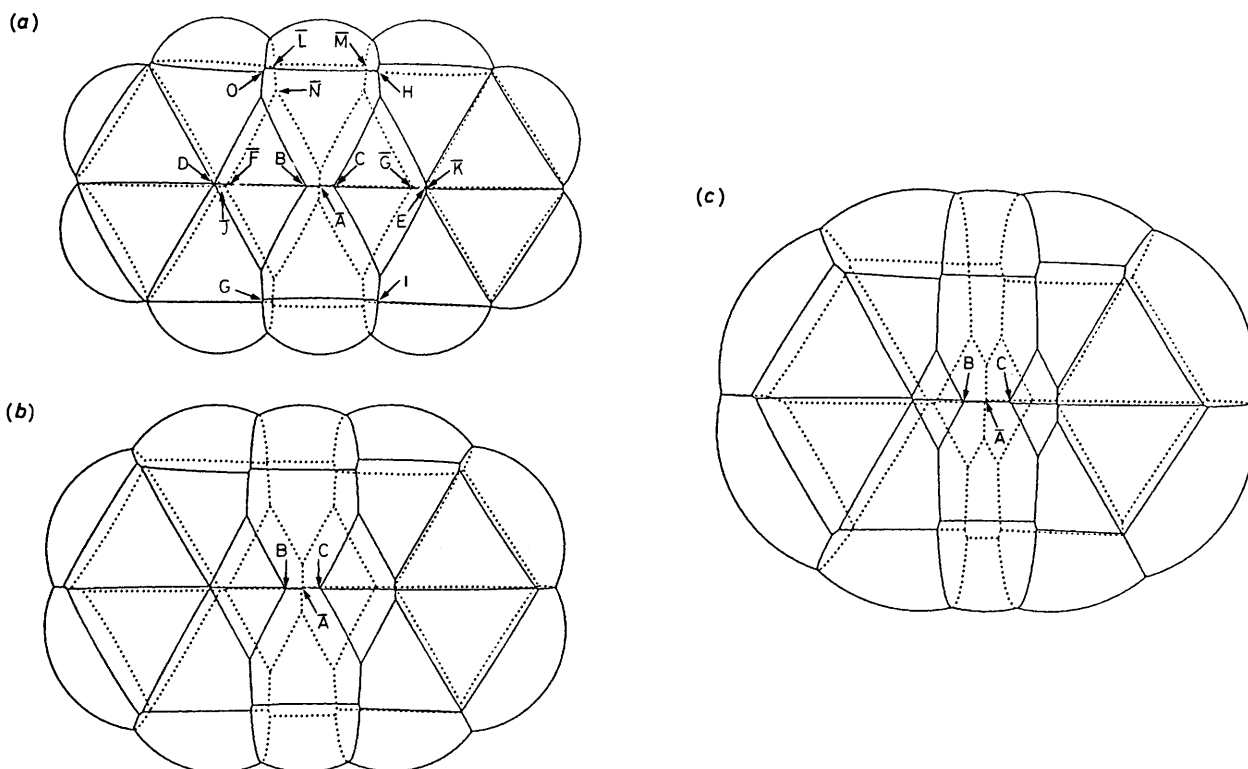


Figure 3. Ion pair surfaces and associated HSE minima for the Li^+ , Cs^+ , and SS^+ ion pairs of anthracene $^{2-}$. The terms used are explained in the headings to Figures 1 and 2. The geometry employed has no symmetry.

Anthracene $^{2-}$, Li^+ [Figure 3(a)] HMO charge distribution; minimum at \bar{A} , 227.8; local minima at B, C, 225.6; D, 203.0; E, 202.9; F, 202.2; \bar{G} , 201.9; further local minima not checked. *Anthracene $^{2-}$, 2Li^+* [Figure 3(a)] (i) HMO charge distribution, minimum at $\bar{A}-\bar{B}$, $\bar{A}-\bar{C}$, 364.0; local minima at C-F ($\approx \bar{B}-\bar{G}$) 356.4; $\bar{A}-\bar{D}$ ($\approx \bar{A}-\bar{E}$) 353.9; F-E ($\approx \bar{D}-\bar{G}$) 350.1; D-E ($\approx \bar{F}-\bar{G}$) 341.0; B-H (≈ 7 almost equivalent sites) 321.7; H-I (≈ 3 almost equivalent sites) 314.9; further local minima not checked. (ii) CNDO-2 charge distribution, minimum at E-J ($\approx \bar{D}-\bar{K}$) 319.3; local minima at B-K ($\approx \bar{C}-\bar{J}$) 314.1; I-L (≈ 3 almost equivalent sites) 313.0; $\bar{A}-\bar{E}$ ($\approx \bar{A}-\bar{D}$) 310.4; D-E ($\approx \bar{J}-\bar{K}$) 310.3; $\bar{M}-\bar{I}$ (≈ 3 almost equivalent sites) 310.2; C-N (≈ 7 almost equivalent sites) 309.8; further local minima not checked. *Anthracene $^{2-}$, Cs^+* [Figure 3(b)] HMO charge distribution, absolute minimum at \bar{A} , 169.0; local minima at B, C, 166.1; further local minima not checked. *Anthracene $^{2-}$, 2Cs^+* [Figure 3(b)] HMO charge distribution, absolute minimum at $\bar{A}-\bar{B}$, $\bar{A}-\bar{C}$, 282.5; local minima not checked. *Anthracene $^{2-}$, SS^+* [Figure 3(c)] HMO charge distribution, minimum at \bar{A} , 101.5; local minima at B, C, 99.6; further local minima not checked. *Anthracene $^{2-}$, 2SS^+* [Figure 3(c)] HMO charge distribution, minimum at $\bar{A}-\bar{B}$, $\bar{A}-\bar{C}$, 173.9; local minima not checked. *Anthracene $^{2-}$, Li^+Cs^+* [Figures 3(a) and (b)] HMO charge distribution, minimum at \bar{A} [Figure 3(a)]-C [Figure 3(b)], $\bar{A}-\bar{B}$, 327.6; local minima not checked. *Anthracene $^{2-}$, Li^+SS^+* [Figures 3(a) and (c)] HMO charge distribution, minimum at \bar{A} [Figure 3(a)]-C [Figure 3(c)], $\bar{A}-\bar{B}$, 285.7; local minima not checked.

the hydrocarbon itself.¹¹ The resultant ion-pair surfaces and the locations of the minima found are shown in Figure 4. As in the case of anthracene dianion there is a very large number of apparent local minima for the dilithium salt which span quite a small energy range, and the ordering of these depends on whether HMO or CNDO-II charge distributions are used. Direct comparison with Sygula's results is difficult since the HSE calculations find many 'minima' which these authors do not seem to have considered. So far as the structural types represented by formulae (10)–(15) is concerned, however, an HMO charge distribution ranks them in the order (13) > (10) > (11) > (12), whereas a CNDO-II charge distribution ranks them in the order (11) > (10) > (13) > (12).

The Acenaphthalene Dianion.—The X-ray crystal structure of [acenaphthalene $^{2-}$, 2Li^+ , $2\text{Me}_2\text{NCH}_2\text{CH}_2\text{NMe}_2$] has been reported by Stucky and co-workers.¹² In this structure, one lithium is above the five-membered ring and the other is below the same ring [equivalent to position $\bar{A}-\bar{A}$ in Figure 5(a)]. Freeman¹³ has, however, suggested a structure, in solution, in which one ion is above the five-membered ring and the other is below a six-membered ring [roughly equivalent to position $\bar{A}-\bar{B}$, in Figure 5(a)]. A somewhat similar structure [roughly equivalent to position $\bar{A}-\bar{C}$ in Figure 5(a)] was suggested by

Edlund and Eliasson¹⁴ on the basis of NMR studies although these authors suggested that the counterion associated with the six-membered ring(s) may be of the solvent-separated type or at least less strongly bound.

The main minima predicted by the HSE calculations are, indeed, of these types. The geometry chosen for the dianion was that of Stucky and co-workers and the resultant ion-pair surfaces and structures are displayed in Figure 5. For a single counterion and an HMO charge distribution, local minima are found over each of the rings. For two Cs^+ or SS^+ counterions the predicted structure of the triple ion is analogous to that of Stucky's crystal structure. If one or both of the counterions is Li^+ , structures analogous to those of Freedman and Edlund are predicted to be more stable.

As well as dianions derived from polynuclear aromatic compounds, dianions based on both classical and non-Kekulé polyenes¹⁵ are well known.^{3–5} We have not attempted a systematic survey of these but have carried out HSE calculations on the stilbene and hexatriene dianions since these are two for which X-ray crystal structures are available.

The Stilbene Dianion.—The X-ray crystal structures of [stilbene $^{2-}$, 2Li^+ , $2\text{Me}_2\text{NCH}_2\text{CH}_2\text{NMe}_2$] and [stilbene $^{2-}$, 2Li^+ , $2\text{Me}_2\text{NCH}_2\text{CH}_2\text{NMeCH}_2\text{CH}_2\text{NMe}_2$] have been

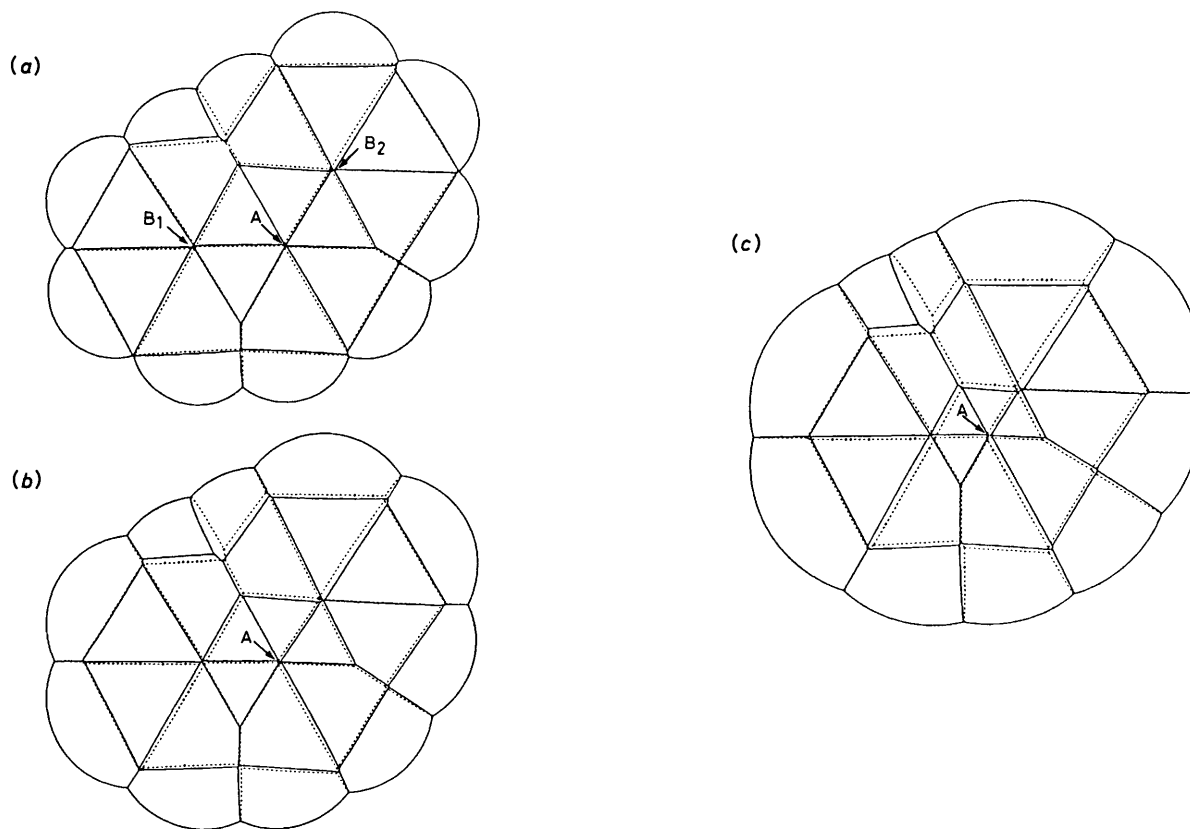


Figure 4. Ion pair surfaces and associated HSE minima for the Li^+ , Cs^+ , and SS^+ ion pairs of phenanthrene $^{2-}$. The terms used are explained in the headings to Figures 1 and 2. Since the anion is almost planar \bar{A} lies almost directly below A.

Phenanthrene $^{2-}$, Li^+ [Figure 4(a)] HMO charge distribution, minimum at A ($\approx \bar{A}$) 234.0; local minima at B_1 (≈ 3 almost equivalent sites) 203.3; further local minima not checked. *Phenanthrene* $^{2-}$, 2Li^+ [Figure 4(a)] (i) HMO charge distribution, minimum at A- \bar{A} , 374.7; local minima at A- \bar{B}_1 (≈ 3 almost equivalent sites) 360.4; B_1 - \bar{B}_2 ($\approx B_2$ - \bar{B}_1) 346.6; many further local minima not checked. (ii) CNDO-2 charge distribution, minimum at B_1 - \bar{B}_2 ($\approx B_2$ - \bar{B}_1) 308.4; local minima at A- \bar{B}_1 (≈ 3 almost equivalent sites) 302.7; many further local minima not checked. *Phenanthrene* $^{2-}$, Cs^+ [Figure 4(b)] HMO charge distribution, minimum at A ($\approx \bar{A}$) 171.4; local minima not checked. *Phenanthrene* $^{2-}$, 2Cs^+ [Figure 4(b)] HMO charge distribution, minimum at A- \bar{A} , 288.9; local minima not checked. *Phenanthrene* $^{2-}$, SS^+ [Figure 4(c)] HMO charge distribution, minimum at A ($\approx \bar{A}$) 101.9; no local minima. *Phenanthrene* $^{2-}$, 2SS^+ [Figure 4(c)] HMO charge distribution, minimum at A- \bar{A} , 176.1; no local minima. *Phenanthrene* $^{2-}$, Li^+ , Cs^+ [Figures 4(a) and (b)] HMO charge distribution, minimum at A [Figure 4(a)]- \bar{A} [Figure 4(b)], \bar{A} -A, 337.2; local minima not checked. *Phenanthrene* $^{2-}$, Li^+ , SS^+ [Figures 4(a) and (c)] HMO charge distribution, minimum at A [Figure 4(a)]- \bar{A} [Figure 4(c)], \bar{A} -A, 293.4; local minima not checked.

reported by Walczak and Stucky. 16 In the former case the lithium cations occupy essentially η^2 sites, centrally placed above and below the central olefinic carbon-carbon bond. In the bis-triamine complex, however, they are slightly displaced towards η^3 sites [approaching A_1 - \bar{A}_2 in Figure 6(a)], giving a structure which, in some ways, resembles a dimer of $\{\text{benzyl}^-, \text{Li}^+, \text{N}[\text{CH}_2\text{CH}_2]_3\text{N}\}_\infty$. 17

For the HSE calculations Stucky's geometry was used for the dianion and the resultant ion-pair surfaces and HSE minima are shown in Figure 6. For a single counterion (Li^+ , Cs^+ , or SS^+) the result is very close to that in benzyl-lithium with the counterion located in an η^3 site (A_1 , A_2 , \bar{A}_1 , or \bar{A}_2 in Figure 6) bridging the benzyl/ α - and *ortho*-carbon atoms. For a single lithium cation, minima are also found with the counterion over the benzene rings. The minima found for two counterions are combinations of these sites. No minimum is found corresponding to that on the crystalline bis- $\text{Me}_2\text{NCH}_2\text{CH}_2\text{NMe}_2$ complex of the lithium salt but the energy surface for conversion of the structure A_1 - \bar{A}_2 [Figure 6(a)] into \bar{A}_1 - A_2 which passes through an equivalent structure is very flat so that formation of a structure does not appear in any way surprising.

The Hexatriene Dianion.—The hexatriene dianion can adopt six different planar conformations. In the crystalline complex

[hexatriene $^{2-}$, 2Li^+ , $2\text{Me}_2\text{NCH}_2\text{CH}_2\text{NMe}_2$] the hexatriene unit is *cis*(bond C-2-C-3)-*trans*(C-3-C-4)-*cis*(C-4-C-5). 18 The carbon skeleton is not quite planar. One lithium cation bridges atoms C-1, C-2, C-3, and C-4 whereas the other, on the opposite face, bridges atoms C-3, C-4, C-5, and C-6 [close to structure A- \bar{A} in Figure 7(a)], giving a structure which has been described as a dimer of allyl-lithium.

For the HSE calculations the geometry used for the hexatriene was that of Arora *et al.* 18 and the resultant ion-pair surfaces and HSE minima are shown in Figure 7. A single counterion (Li^+ , Cs^+ , or SS^+) is found to adopt η^3 sites analogous to the situation in allyl-lithium, 1 whereas for two counterions structures are predicted to be analogous to that found by Arora. 18

Radical Anions.—At the HMO level of approximation, for an alternant hydrocarbon, $(q_i)^{2-}$ (the charge at the i 'th atom in the dianion) is twice $(q_i)^{-}$ (the charge at the i 'th atom in the radical anion). Hence the ion-pairing surfaces for benzene $^{2-}$, M^+ (Figure 1); naphthalene $^{2-}$, M^+ (Figure 2); anthracene $^{2-}$, M^+ (Figure 3); phenanthrene $^{2-}$, M^+ (Figure 4); stilbene $^{2-}$, M^+ (Figure 6); and hexatriene $^{2-}$, M^+ (Figure 7) are simply scaled versions of the surfaces for the corresponding radical anions.

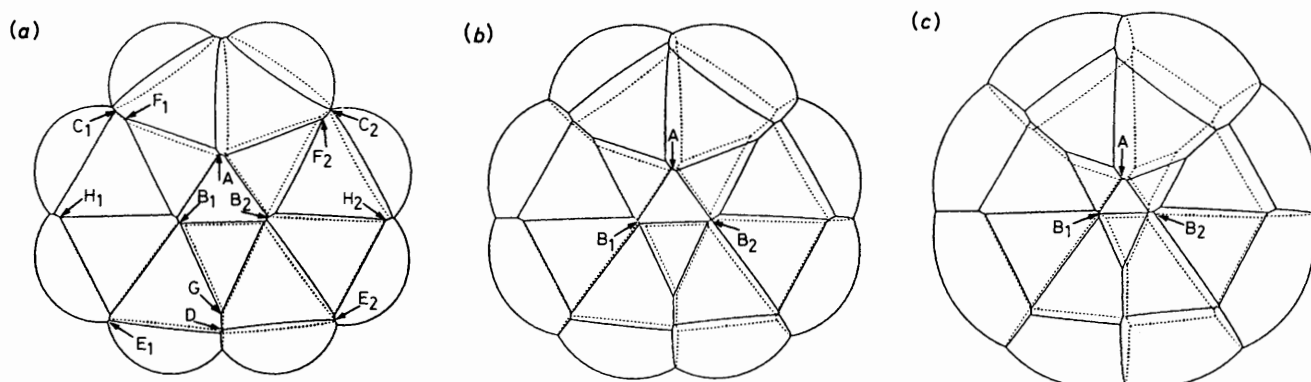


Figure 5. Ion-pair surfaces and associated HSE minima for the Li^+ , Cs^+ , and SS^+ ion pairs of acenaphthalene $^{2-}$. The terms used are explained in the headings to Figures 1 and 2. Since the anion is almost planar \bar{A} lies almost directly beneath A. In all cases HMO charge distributions were used.

Acenaphthalene $^{2-}$, Li^+ [Figure 5(a)] minimum at A ($\approx \bar{A}$) 232.5; local minima at B_1 ($B_2, \bar{B}_1, \bar{B}_2$) 224.8; no further local minima. *Acenaphthalene* $^{2-}$, 2Li^+ [Figure 5(a)] minimum at $A-\bar{B}_1$ ($\approx A-\bar{B}_2, \bar{A}-\bar{B}_1, \bar{A}-\bar{B}_2$) 381.2; local minima at $A-\bar{A}$, 379.9; $B_1-\bar{B}_2$ ($\approx \bar{B}_1-\bar{B}_2$) 374.5; $C_1-\bar{B}_2$ ($\approx C_2-\bar{B}_1, \bar{C}_1-\bar{B}_2, \bar{C}_2-\bar{B}_2$) 351.3; $A-\bar{D}$ ($\bar{A}-\bar{D}$) 345.0; $A-\bar{E}_2$ ($\approx A-\bar{E}_1, \bar{A}-\bar{E}_1, \bar{A}-\bar{E}_2$) 327.7; $F_1-\bar{F}_2$ ($\approx F_1-\bar{F}_2$) 325.9; $G-\bar{F}_2$ ($\approx G-\bar{F}_1, \bar{G}-\bar{F}_1, \bar{G}-\bar{F}_2$) 323.2; $H_1-\bar{B}_2$ ($\approx H_2-\bar{B}_1, \bar{H}_1-\bar{B}_2, \bar{H}_2-\bar{B}_1$) 321.2; $H_1-\bar{A}$ ($\approx H_2-\bar{A}, \bar{H}_1-\bar{A}, \bar{H}_2-\bar{A}$) 318.2; $B_1-\bar{E}_2$ ($\approx B_2-\bar{E}_1, \bar{B}_1-\bar{E}_2, \bar{B}_2-\bar{E}_1$) 315.5; no further local minima. *Acenaphthalene* $^{2-}$, Cs^+ [Figure 5(b)] minimum at A ($\approx \bar{A}$) 170.7; local minima at B_1 ($B_2, \bar{B}_1, \bar{B}_2$) 168.2; no further local minima. *Acenaphthalene* $^{2-}$, 2Cs^+ [Figure 5(b)] minimum at $A-\bar{A}$, 289.3; local minima not checked. *Acenaphthalene* $^{2-}$, SS^+ [Figure 5(c)] minimum at A ($\approx \bar{A}$) 107.8; local minima at B_1 ($\approx B_2, \bar{B}_1, \bar{B}_2$) 101.3; no further local minima. *Acenaphthalene* $^{2-}$, 2SS^+ [Figure 5(c)] minimum at $A-\bar{A}$, 176.3; local minima not checked. *Acenaphthalene* $^{2-}$, Li^+ , Cs^+ [Figures 5(a) and (b)] minimum at A [Figure 5(a)]- \bar{B}_1 [Figure 5(b)], $A-\bar{B}_2, \bar{A}-\bar{B}_1, \bar{A}-\bar{B}_2$, 339.9; local minima not checked. *Acenaphthalene* $^{2-}$, Li^+ , SS^+ [Figures 5(a) and (c)] minimum at A [Figure 5(a)]- \bar{B}_1 [Figure 5(c)], $A-\bar{B}_2, \bar{A}-\bar{B}_1, \bar{A}-\bar{B}_2$, 293.7; local minima not checked.

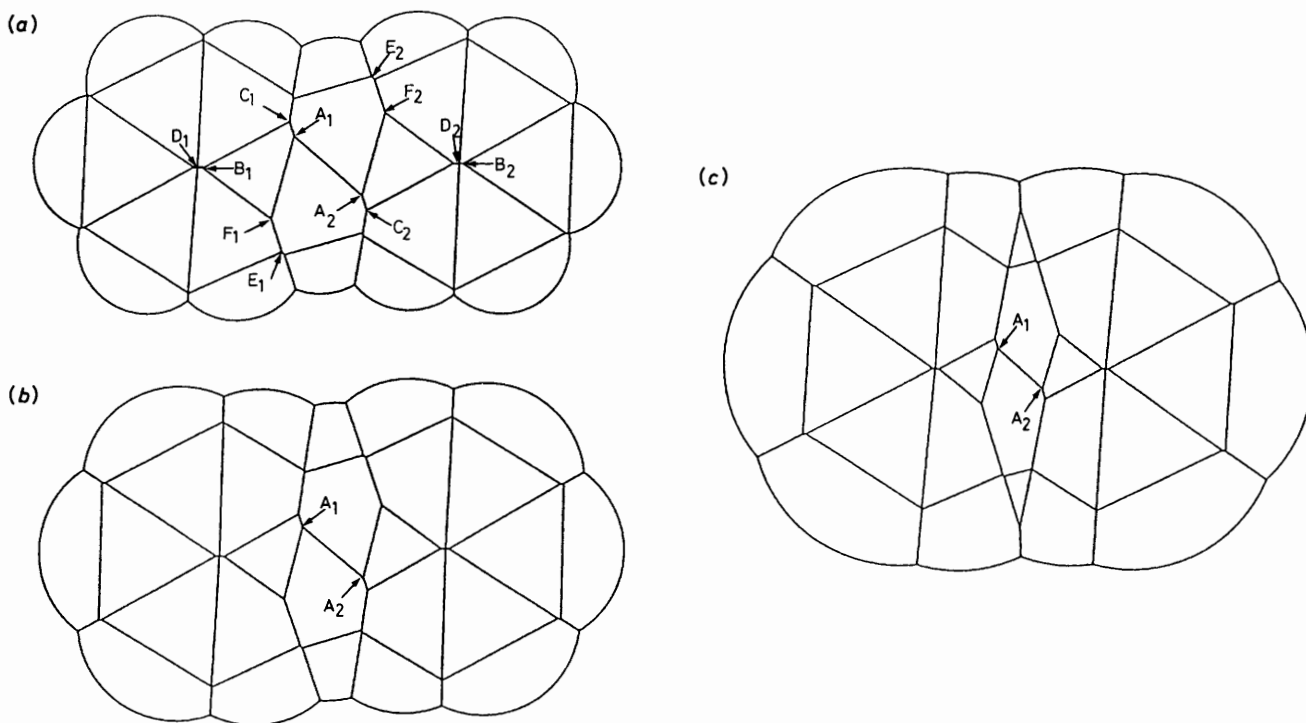


Figure 6. Ion-pair surfaces and associated HSE minima for the Li^+ , Cs^+ , and SS^+ ion pairs of stilbene $^{2-}$. The terms used are explained in the headings to Figures 1 and 2. Since the anion is planar \bar{A}_1 lies directly beneath A_1 . In all cases HMO charge distributions were used.

Stilbene $^{2-}$, Li^+ [Figure 6(a)] minimum at $A_1, A_2, \bar{A}_1, \bar{A}_2$, 224.1; local minima at $B_1, B_2, \bar{B}_1, \bar{B}_2$, 188.3; no further local minima. *Stilbene* $^{2-}$, 2Li^+ [Figure 6(a)] minimum at $A_1-\bar{A}_2, \bar{A}_1-\bar{A}_2$, 370.8; local minima at $A_1-\bar{B}_2, A_2-\bar{B}_1, \bar{A}_1-\bar{B}_2, \bar{A}_2-\bar{B}_1$, 352.2; $C_1-\bar{D}_2, C_2-\bar{D}_1, \bar{C}_1-\bar{D}_2, \bar{C}_2-\bar{D}_1$, 334.6; $C_1-\bar{C}_2, \bar{C}_1-\bar{C}_2$, 340.0; $E_1-\bar{E}_2, \bar{E}_1-\bar{E}_2$, 327.6; $D_1-\bar{D}_2, \bar{D}_1-\bar{D}_2$, 324.5; $D_1-\bar{F}_2, D_2-\bar{F}_1, \bar{D}_1-\bar{F}_2, \bar{D}_2-\bar{F}_1$, 324.3; no further local minima. *Stilbene* $^{2-}$, Cs^+ [Figure 6(b)] minimum at $A_1, A_2, \bar{A}_1, \bar{A}_2$, 164.8; no local minima. *Stilbene* $^{2-}$, 2Cs^+ [Figure 6(b)] minimum at $A_1-\bar{A}_2, \bar{A}_1-\bar{A}_2$, 279.4; local minima not checked. *Stilbene* $^{2-}$, SS^+ [Figure 6(c)] minimum at $A_1, A_2, \bar{A}_1, \bar{A}_2$, 99.5; no local minima. *Stilbene* $^{2-}$, 2SS^+ [Figure 6(c)] minimum at $\bar{A}_1-\bar{A}_2, A_1-\bar{A}_2$, 172.1; local minima not checked. *Stilbene* $^{2-}$, Li^+ , Cs^+ [Figures 6(a) and (b)] minimum at A_1 [Figure 6(a)]- \bar{A}_2 [Figure 6(b)], $A_2-\bar{A}_1$, 327.7; local minima not checked. *Stilbene* $^{2-}$, Li^+ , SS^+ [Figures 6(a) and (c)] minimum at A_1 [Figure 6(a)]- \bar{A}_2 [Figure 6(c)], $\bar{A}_1-\bar{A}_2$, 283.1; local minima not checked.

The energies for the HSE minima should just be divided by two. Note, however, that since acenaphthalene is non-alternant the surface for acenaphthalene $^{2-}$ cannot be inferred from that of the dianion and for none of the systems can the surface for R^{2-} , 2M^+

be inferred from that of R^{2-} , 2M^+ (since a simple division by two halves the cation/cation repulsion).

Despite the extensive literature on the ESR spectroscopy of radical anions most evidence on the structures of ion pairs is

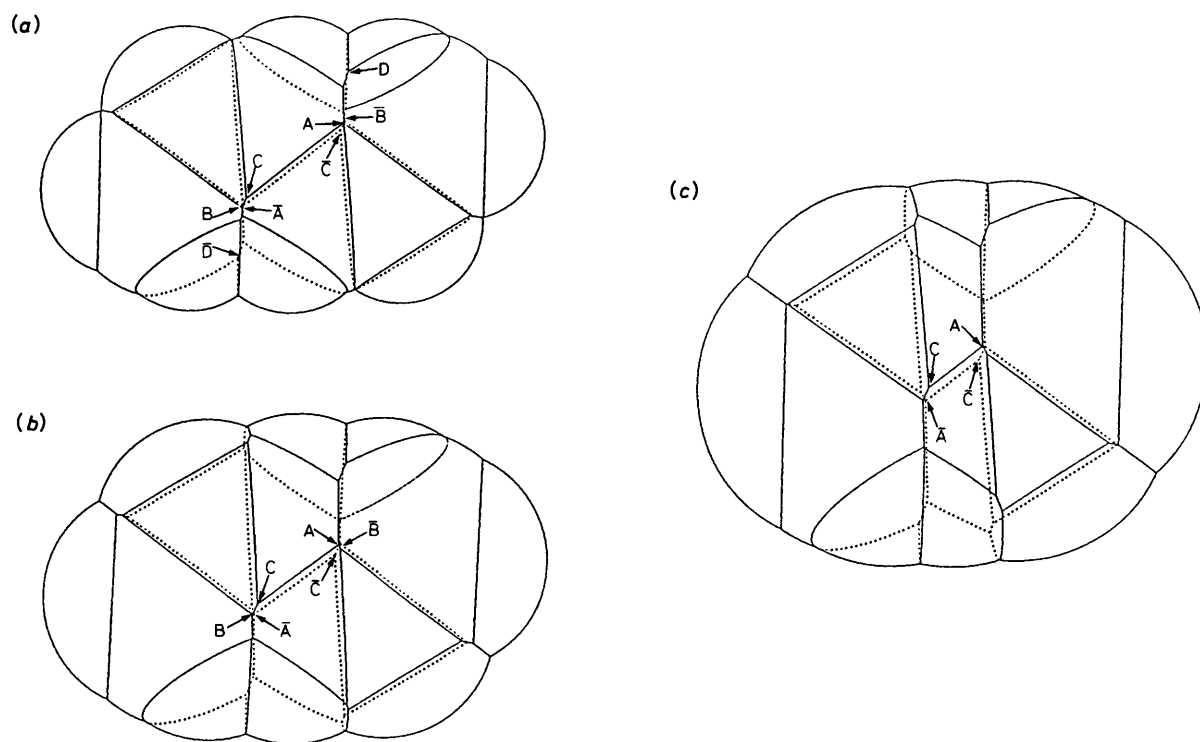


Figure 7. Ion-pair surfaces and associated HSE minima for the Li^+ , Cs^+ , and SS^+ ion pair surfaces of hexatriene $^{2-}$. The terms used are explained in the headings to Figures 1 and 2. The anion has an inversion centre at the middle of the C3–C4 bond. \bar{A} is related to A via this symmetry element.

Hexatriene $^{2-}$, Li^+ [Figure 7(a)] HMO charge distribution, minimum at A, \bar{A} , 196.8; local minimum at B, \bar{B} , 195.3; no further local minima. Hexatriene $^{2-}$, 2Li^+ [Figure 7(a)] (i) HMO charge distribution, minimum at B– \bar{B} , 314.5; local minimum at A– \bar{C} , \bar{A} –C, 292.9; no further local minima. (ii) CNDO-2 charge distribution, minimum at B– \bar{B} , 398.5; local minima at B–D, \bar{B} –D, 373.6; A–C, \bar{C} –A, 373.3; no further local minima. Hexatriene $^{2-}$, Cs^+ [Figure 7(b)] HMO charge distribution, minimum at A, \bar{A} , 138.5; local minimum at B, \bar{B} , 137.7; no further local minima. Hexatriene $^{2-}$, 2Cs^+ [Figure 7(b)] HMO charge distribution, minimum at B– \bar{B} , 225.8; local minimum at A–C, \bar{A} –C, 221.4; no further local minima. Hexatriene $^{2-}$, SS^+ [Figure 7(c)] HMO charge distribution, minimum at A, \bar{A} , 80.3; local minimum at C, \bar{C} , 80.2; no further local minima. Hexatriene $^{2-}$, 2SS^+ [Figure 7(c)] HMO charge distribution, minimum at A– \bar{A} , 133.7; local minimum at A–C, \bar{A} –C, 133.0; no further local minima. Hexatriene $^{2-}$, Li^+ , Cs^+ [Figures 7(a) and (b)] HMO charge distribution, minimum at A [Figure 7(a)]– \bar{A} [Figure 7(b)], \bar{A} –A, 274.0; local minima not checked. Hexatriene $^{2-}$, Li^+ , SS^+ [Figures 7(a) and (c)] HMO charge distribution, minimum at A [Figure 7(a)]– \bar{A} [Figure 7(c)], 236.3; local minima not checked.

indirect and only a few radical anions 19 give crystalline derivatives suitable for X-ray crystallographic investigation.

ESR studies of the potassium, rubidium, and caesium salts of benzene radical anion are taken to indicate a structure in which the metal is η^6 -co-ordinated and centrally placed over the ring. 20 This is in agreement with the HSE results shown in Figure 1.

For naphthalene $^{\cdot-}$, Li^+ , INDO molecular orbital calculations 21 and electrostatics calculations 22 using McClelland's method 23 predict one energy minimum above and below each ring. These agree with the HSE results shown in Figure 2 and also with attempts to fit the ESR spectral hyperfine splittings of (naphthalene $^{\cdot-}$, Li^+) 7 and (naphthalene $^{\cdot-}$, Na^+) 24 although ESR evidence for the lithium salt was originally interpreted in terms of a model in which the lithium was positioned over the central carbon–carbon bond. 25

For anthracene $^{\cdot-}$, Li^+ McClelland-type calculations 22,23 predict a single minimum with the lithium over the central ring. The HSE calculations (Figure 3) also predict this to be the major minimum but with local minima associated with the outer rings.

Calculations of electrostatic potentials in planes 2.5 Å and 7 Å above a planar phenanthrene radical anion 26 suggest a central minimum at 7 Å but not 2.5 Å. It is, however, very difficult to predict ion-pair structures from this type of calculation unless a very large number of planes are examined and steric exclusion volumes plotted within each plane. 2,27 The HSE results are uncomplicated (Figure 4) and show the

minimum as being associated with the central ring with local minima over the outer rings.

Structures for the ion pairs of stilbene and hexatriene radical anions can be inferred from Figures 5 and 6 but as far as we are aware there is no independent evidence against which these predications can be checked.

Dications and Radical Cations.—At the HMO level of approximation, for an alternant hydrocarbon, $(q_i)^{2+}$ (the charge at the i 'th carbon in a dication) is the mirror image of $(q_i)^{2-}$ (the equivalent charge in the dianion) and $(q_i)^{+}$ is the mirror image of $(q_i)^{-}$. Hence the results for ion pairs of most of the dianions and radical anions discussed in this paper (except acenaphthalene) can be taken as a first-order guide to the ion-pairing behaviour of the corresponding cations! Unfortunately, little is known of the structures of such dication and radical cation ion pairs that would provide data for the purposes of comparison.

Conclusions.—The aim of this paper and four of the preceding papers 1,2,27,28 has been to explore the extent to which a simple electrostatic method could successfully model the structures and reactions of group 1 organometallic ion pairs and to develop a method that could be used to predict structures for ion pairs for which such information is otherwise difficult to obtain. In doing so we have stressed that electrostatic methods based on potentials in planes through molecules or parallel to

the molecular plane are totally unreliable and that the significant surface in such calculations is the ion-pair surface.

Although the HSE method proves generally successful in predicting ion-pair structures, there are problems with some systems where it is found that the HSE prediction does not accord with those obtained by other methods and the HSE prediction itself becomes dependent on what MO method is used to produce the anion atomic charges. These problems do not occur in the majority of systems. In these there are relatively few local energy minima and these are well spaced. In these cases the results are similar whichever HSE charge distribution is used. They correlate in a qualitative fashion with the results of MO calculations and known X-ray crystal structures. In such cases clear inferences can be drawn as to the structure of the major ion pair in solution. Problems arise, however, in those systems where there are many local minima which cover only a small spread of energies (e.g., anthracene²⁻, 2Li⁺ and phenanthrene²⁻, 2Li⁺) or where, by chance, there are two types of energy minima which are close to each other (e.g., benzyl⁻, Li⁺).¹ In such cases it would be rash to claim that an HSE calculation, an MO calculation, or even an X-ray crystal structure provides a reliable guide to the structure(s) in solution.

Comparison of the results for monoanions¹ and those for the dianions discussed in the present paper produces an interesting contrast. In the case of the monoanions the positions adopted by the cations in the triple ion R⁻, 2Li⁺ rarely relate to the minimum-energy sites found in the 1:1 ion pairs R⁻, Li⁺. However, for the dianions the main positions adopted by the cations in the triple ions R²⁻, 2Li⁺ are often simple combinations of those found in the 1:1 ion pairs R²⁻, Li⁺. This difference in behaviour seems to reflect the relative importance of cation/cation repulsion and cation/anion attractive terms in the two sorts of triple ions, the repulsive term being relatively more important in R⁻, 2Li⁺.

Acknowledgements

We thank the SERC for financial support.

References

- 1 Part 11, R. J. Bushby, H. L. Steel, and M. P. Tytko, preceding paper.
- 2 R. J. Bushby and H. L. Steel, Part 10, *J. Chem. Soc., Perkin Trans. 2*, this issue.
- 3 R. H. Nobes, D. Poppinger, W.-K. Li, and L. Radom, in

- 'Comprehensive Carbanion Chemistry Part C,' eds. E. Buncl and T. Durst, Elsevier, Amsterdam, 1987.
- 4 E. Grovenstein, in ref. 3.
- 5 R. B. Bates, in 'Comprehensive Carbanion Chemistry Part A,' eds. E. Buncl and T. Durst, Elsevier, Amsterdam, 1980; J. Klein, *Tetrahedron*, 1983, **39**, 2733.
- 6 A. Streitwieser and J. T. Swanson, *J. Am. Chem. Soc.*, 1983, **105**, 2502.
- 7 J. J. Brooks, W. Rhine, and G. D. Stucky, *J. Am. Chem. Soc.*, 1972, **94**, 7346.
- 8 A. Sygula, K. Lipkowitz, and P. W. Rabideau, *J. Am. Chem. Soc.*, 1987, **109**, 6602.
- 9 W. E. Rhine, J. Davis, and G. Stucky, *J. Am. Chem. Soc.*, 1975, **97**, 2079.
- 10 C. Raston and G. Salem, *J. Chem. Soc., Chem. Commun.*, 1984, 1702.
- 11 M. I. May, Y. Okaya, and D. E. Cox, *Acta Crystallogr., Ser. B*, 1971, **26**, 27.
- 12 W. E. Rhine, J. H. Davis, and G. D. Stucky, *J. Organomet. Chem.*, 1977, **134**, 139.
- 13 H. H. Freeman, A. C. S. Meeting, Sept. 1971, Abstracts ORGN80.
- 14 B. Eliasson and U. Edlund, *J. Chem. Soc., Perkin Trans. 2*, 1983, 1837.
- 15 R. J. Bushby and C. Jarecki, *Tetrahedron Lett.*, 1988, **29**, 2715.
- 16 W. Walczak and G. Stucky, *J. Organomet. Chem.*, 1975, **97**, 313; *J. Am. Chem. Soc.*, 1976, **98**, 5531.
- 17 S. P. Patterman, I. L. Karle, and G. D. Stucky, *J. Am. Chem. Soc.*, 1970, **92**, 1150.
- 18 S. K. Arora, R. B. Bates, W. A. Beavers, and R. S. Cutler, *J. Am. Chem. Soc.*, 1975, **97**, 6271.
- 19 J. J. Mooij, A. A. K. Klaasen, E. de Boer, H. M. L. Degens, T. E. M. van den Hark, and J. H. Noordik, *J. Am. Chem. Soc.*, 1976, **98**, 680; J. H. Noordik, H. M. Doesburg, and P. A. J. Prick, *Acta Crystallogr., Sect. B*, 1981, **37**, 1659.
- 20 M. T. Jones and T. C. Kuechler, *J. Phys. Chem.*, 1977, **81**, 360.
- 21 B. L. Pedersen and R. G. Griffin, *Chem. Phys. Lett.*, 1970, **5**, 373.
- 22 I. B. Goldberg and J. R. Bolton, *J. Phys. Chem.*, 1970, **74**, 1965.
- 23 B. J. McClelland, *Chem. Rev.*, 1964, **64**, 301.
- 24 G. W. Canters, C. Corvaja, and E. de Boer, *J. Chem. Phys.*, 1971, **54**, 3026.
- 25 M. Iwaizumi, M. Suzuki, T. Isobe, and H. Azumi, *Bull. Chem. Soc. Jpn.*, 1968, **41**, 732.
- 26 M. T. Jones and R. H. Ahmed, *J. Phys. Chem.*, 1980, **84**, 2913.
- 27 R. J. Bushby and M. P. Tytko, *J. Organomet. Chem.*, 1984, **270**, 265.
- 28 R. J. Bushby and H. L. Steel, *J. Organomet. Chem.*, 1987, **336**, C25.
- 29 G. D. Stucky, *Adv. Chem. Ser.*, 1974, **130**, 56.

Paper 9/04101J

Received 25th September 1989

Accepted 7th February 1990